Tina Memo No. 2007-009
Internal Memo

Dependency of the TINA DODECANTS Algorithm on Scanner Manufacturer and Slice Orientation

P. A. Bromiley

Last updated
20 / 8 / 2007

Imaging Science and Biomedical Engineering Division,
Medical School, University of Manchester,
Stopford Building, Oxford Road,
Manchester, M13 9PT.

Dependency of the TINA DODECANTS Algorithm on Scanner Manufacturer and Slice Orientation

P. A. Bromiley
Dept. of Medical Biophysics
Imaging Science and Biomedical Engineering Division
Medical School, University of Manchester
Manchester, M13 9PT, UK
paul.bromiley@man.ac.uk

Abstract

This report describes the application of the TINA DODECANTS algorithm to multiple MRI image volumes from the same subject, acquired using different slice orientations and different scanners. Coronal and axial inversion recovery MR image volumes of the head were obtained from a single normal volunteer, using two 1.5T MRI scanners from different manufacturers. The TINA DODECANTS algorithm was then applied to measure the cerebrospinal fluid (CSF) volume in each image volume, and the results compared to previous measurements described in TINA Memo no. 2004-002. The comparison indicated that the variation in CSF volume with slice direction is minimal, but that the measured volume could vary by up to a factor of 2 across different scanners. We therefore conclude that, whilst the technique can be used to study variations across image volumes from multiple subjects acquired using the same scanner and scan parameters, image volumes from multiple scanners cannot be reliably combined into a single study.

1 Method

1.1 CSF Volume Measurement

Six MRI volumes were obtained from a normal female volunteer (age=27), using the parameters given in Table 1; axial and coronal volumes were obtained using each set of parameters. Analysis of the image data was performed using the TINA medical image analysis software (www.tina-vision.net) and consisted of three stages. First, all image volumes were registered to the TINA standard image volume (www.tina-vision.net/tarballs/DODECANTS) using a technique based on maximum likelihood alignment of edges. Second, the TINA segmentation algorithm, based on fitting a partial volume model of the tissues present in the head to the histogram of the image volumes [14, 13, 16], was used to segment the CSF. In order to reduce the processor time required, two cuboidal regions were defined in the standard coordinate system, lying within the skull and covering the anterior and posterior six slices containing the ventricles. The combined region contained only grey matter, white matter and CSF, and could therefore be described using a model consisting of only three tissues, comprising Gaussian components to represent the pure tissues, and triangular distributions convolved with Gaussians to represent the partial volume contributions for all three pairs of tissues. Each component was described by three parameters: a mean grey level, a standard deviation, and a prior term representing the probability of occurrence of the component, giving a total of eighteen parameters. The model was fitted to the histogram of the image volumes using the Expectation-Maximisation algorithm. Volumetric maps of the CSF distribution were then produced from the models, and binarised at the 0.5 probability threshold to produce a CSF segmentation. The segmented images were then multiplied with a set of binary masks produced in the standard coordinate system. The masking had two purposes: to delete non-CSF fluid spaces (e.g. eyes, sinuses) and to enforce a consistent inferior boundary to the measurement space, defined by drawing a line in the mid-sagittal section parallel to the horizontal axis that passed through the junction of the calvarium and the tentorium cerebelli. The anterior, posterior, lateral, and superior boundaries of the CSF space were automatically identified by locating the extremes of the CSF. Finally, the number of voxels in the binarised, masked CSF maps was counted and multiplied by the voxel size to produce a measurement of the CSF volume. The CSF volume measurement was performed in the original coordinate system of the images, in order to avoid introducing errors originating from the registration or from any interpolation required to transform the images into the standard coordinate system. Finally, the measurements were normalised to the total intracranial volume (TIV). The TIV was obtained by multiplying the maximal extents of the CSF space in the lateral, anterior-posterior, and

inferior-superior directions in the standard coordinate system to obtain the volume of a bounding box on the CSF space, and then multiplying this volume by the constant of proportionality between CSF bounding box volume and TIV derived in TINA Memo no. 2004-002.

After measurement of the total CSF volumes, the measurement space was divided into twelve eqi-sized cuboidal regions, by defining planes that split the standard coordinate system into lateral halves, inferior and superior halves, and anterior, middle and posterior thirds. The CSF volumes in each of these regions were calculated, and normalised to the TIV in the same way as described above. Again, the CSF volume measurement was performed in the original coordinate system of the images, in order to avoid errors due to interpolation.

Scanner	Philips Interna	Siemens Avanto (lowres)	Siemens Avanto (highres)
Field strength (T)	1.5	1.5	1.5
Repetition time (ms)	6850	6580	4000
Echo time (ms)	18	14	454
Inversion time (ms)	300	350	350
Echo train length	9	9	125
Slice thickness (mm)	3	3	1
Voxel dimensions (mm)	0.898x0.898	0.449x0.449	1.016x1.016
No. voxels	256x256	512x512	224x256

Table 1: Scanner parameters

The TINA segmentation algorithm requires an initial tissue model to act as a starting point for the EM-based optimisation. The intensity histograms of the various image volumes used in this study were similar in shape, but had considerable scaling differences. Therefore, in order to allow the use of a consistent initial model, a mean model was produced from the segmentation models resulting from the study described in TINA Memo no. 2002-004. An initial fitting stage was then performed in which this mean model was scaled to fit the intensity histogram of the axial volume produced using each scanner and set of parameters, using a maximum likelihood based technique. The three resultant models were then used as the initial models for the EM optimisation for both the axial and corresponding coronal scans.

In addition, it should be noted that the Siemens lowres scans, upon inspection, lacked a clear CSF peak in the intensity histogram. The segmentation algorithm was therefore unable to reliably segment the CSF using intensity information alone. The TINA segmentation algorithm has the capability to incorporate gradient information within the feature space, and this facility was used with these scans in order to obtain a reasonable model. However, this problem casts doubt on the suitability of the Siemens lowres modality for use with the TINA DODECANTS technique.

1.2 Analysis of the Results

Analysis of the TIV-normalised CSF volumes was performed through comparison to the results described in TINA Memo no. 2004-002. In that study, the segmentation algorithm was applied to 70 normal volunteers (32 male and 38 female) ranging in age from 19 to 85 years with a mean age of 57 $\pm$ 20 years. All subjects underwent cognitive assessment including the Mini-Mental State Examination (MMSE) to exclude significant cognitive impairment suggestive of undiagnosed dementia [7], and none had vascular risk factors. The local ethics committee approved the research, and informed consent was given for inclusion in the study by the subjects. All subjects underwent MR imaging with a 1.5-T system (ACS-NT, with PowerTrack 6000 gradient subsystem; Phillips Medical Systems, Hamburg, Germany) with a birdcage head coil receiver. Fast spin-echo inversion-recovery images (repetition time, 6850 msec; echo time, 18 msec; inversion time, 300msec; echo train length, 9) were obtained in contiguous 3-mm thick sections throughout the brain, with an in-plane resolution of $0.89mm^2$ (matrix, 256×204, field of view, $230 \times 184mm$), and real image reconstruction was performed. This protocol was essentially the same as the Philips scans acquired in the present study. The segmentation algorithm was applied, as described above, in order to measure the CSF volume in each image volume, and a Weibull cumulative distribution function was fitted to the data in order to obtain the mean and standard deviation of the CSF volume at any given age, where the s.d. represents expected biological variability within a subject group after normalisation for head size differences.

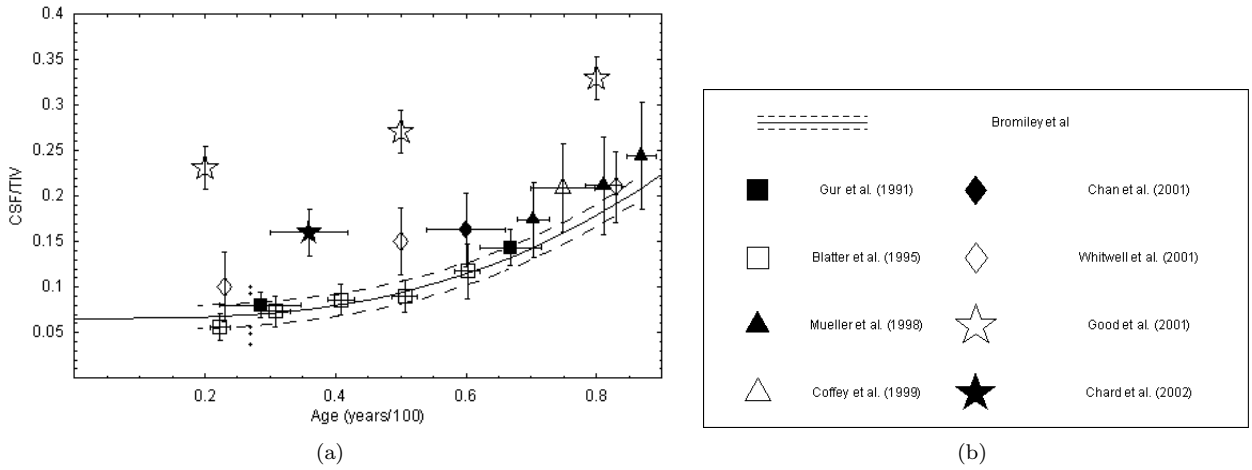

(a) (b)

Figure 1: (a) TIV normalised CSF volume measurements for the single volunteer used in this study (small points) plotted together with the measurements obtained from the papers described in Table 2 and the Weibull CDF fit obtained in TINA Memo no 2004-002: the dashed lines show the upper and lower standard errors. (b) Key to the previous studies.

Reference	No. subjects	Definition of measurement space	Segmentation
Gur et. al. 1991 [10]	69 T	Excludes cerebellum	T2/PD 2D histogram fitting
Blatter et. al. 1995 [2]	89 M 105 F	TIV	ANALYZE [15, 5]
Mueller et. al. 1998 [12]	46 T	Excludes brainstem	REGION [11]
Coffey et. al. 1999 [6]	122 M 198 F	Excludes slices below midbrain	MedVision
Chan et. al. 2001 [3]	10 T	TIV	MIDAS [8]
Whitwell et. al. 2001 [17]	55 T	Excludes slices below cerebellum	MIDAS [8]
Good. et. al. 2001 [9]	265 M 200 F	TIV	SPM99 [1]
Chard et. al. 2002 [4]	13 M 14 F	Excludes slices containing cerebellum	SPM99 [1]

Table 2: Details of the experimental method adopted by studies used in the meta-study, showing the number of subjects included (M=male; F=female; T=total, where the number of each sex was not given), the definition of the measurement space (where TIV is indicated, the whole CSF pool inside the cranium was used), and the software used to perform the segmentation.

In addition, a meta-study was performed in which eight papers published between 1991 and 2002, which quoted TIV and CSF volume measurements from MR images in normal subjects, were used. These previous studies used a variety of MR pulse sequences, definitions of the measurement space, and segmentation routines, summarised in Table 2. The definitions of the measurement space and the segmentation routines used varied considerably between the studies incorporated in the meta-study, and so provided an indication of the expected inter-study variability introduced by changes in protocol and segmentation algorithm.

2 Results

2.1 Total TIV normalised CSF volumes

Figure 1 shows the six TIV normalised CSF volume measurements obtained from the single volunteer used in this study, plotted together with the Weibull CDF fit obtained in TINA Memo no. 2004-002 and the data from the meta-study. Figure 2 shows the current study data in more detail, plotted together with the value interpolated from the Weibull CDF fit at the subject's age and the upper and lower one standard error bars. Numerical interpretation of the intra-scan and inter-study differences is provided in Table 3. The intra-scan differences were evaluated by finding the standard deviation of the TIV normalised CSF volume measurements from the axial and coronal scans from each scanner/set of parameters. These values provide a direct measurement of the repeatability of the segmentation algorithm with changes in slice orientation: since no difference would be expected here, they

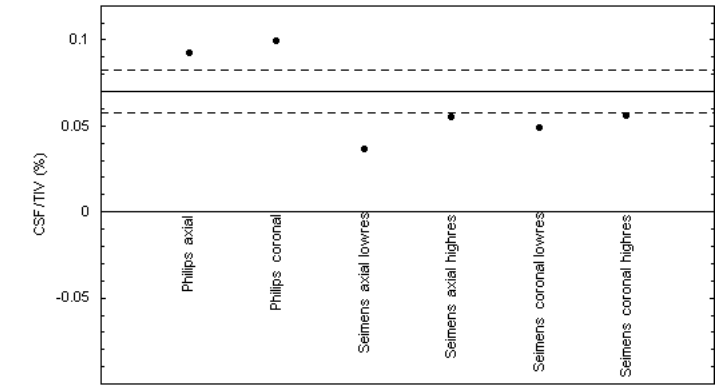

(a)

Figure 2: TIV normalised CSF volume measurements for the single volunteer used in this study plotted together with the expected value from the Weibull CSF fit described in TINA Memo no. 2004-002 (solid line) at the subject's age and the upper and lower standard errors on the fit (dashed lines).

indicate the intrinsic repeatability of the segmentation technique. The inter-study variability was evaluated by finding the mean difference between the TIV normalised CSF volume measurement from the axial and coronal image volumes from each scanner/set of parameters and the expected value at the subject's age interpolated from the Weibull CDF fit described in TINA Memo no. 2004-002. These values indicate the variability introduced into the volume measurement when different protocols are used. In all cases, the data are provided in multiples of the standard error on the Weibull CDF fit at the age of the subject i.e. the expected inter-subject variability that would be seen in large, transverse studies of TIV normalised CSF volume measurement.

Image volume	Intra-scan variability (s.d.'s)	Inter-study variability (s.d.'s)
Philips	0.374	2.067
Siemens lowres	0.694	1.899
Siemens highres	0.043	1.378

Table 3: The intra-scan variability i.e. the differences between the axial and coronal volumes from each scanner/set of parameters and intra-study variability i.e. the mean difference between the axial and coronal volumes from each scanner/set of parameters and the value expected from the Weibull CDF fit described in TINA Memo no. 2004-002, quoted in multiples of the standard deviation derived from that study i.e. the expected level of biological variability in TIV normalised CSF volumes across a group of subjects.

2.2 TIV normalised CSF volumes in the twelve DODECANTS regions

Figures 3 and 4 show the TIV normalised CSF volumes in each of the twelve DODECANTS regions, for each of the image volumes used in the study, plotted together with the expected values based on the Weibull CDF fits described in TINA Memo no. 2004-002. The upper and lower standard errors on the fits are also shown: these define the expected variation across a large group of normal subjects, and so provide an indication of the errors expected in transverse studies. Figure 5 shows the same data, plotted against box number for each image volume, with the abscissa in the form of a Bland-Altman plot i.e. plotted in units of standard deviation. Finally, the same results are given numerically in Table 4, in the form of the mean differences (again in units of the standard error on the Weibull CDF fit) across the twelve DODECANTS boxes.

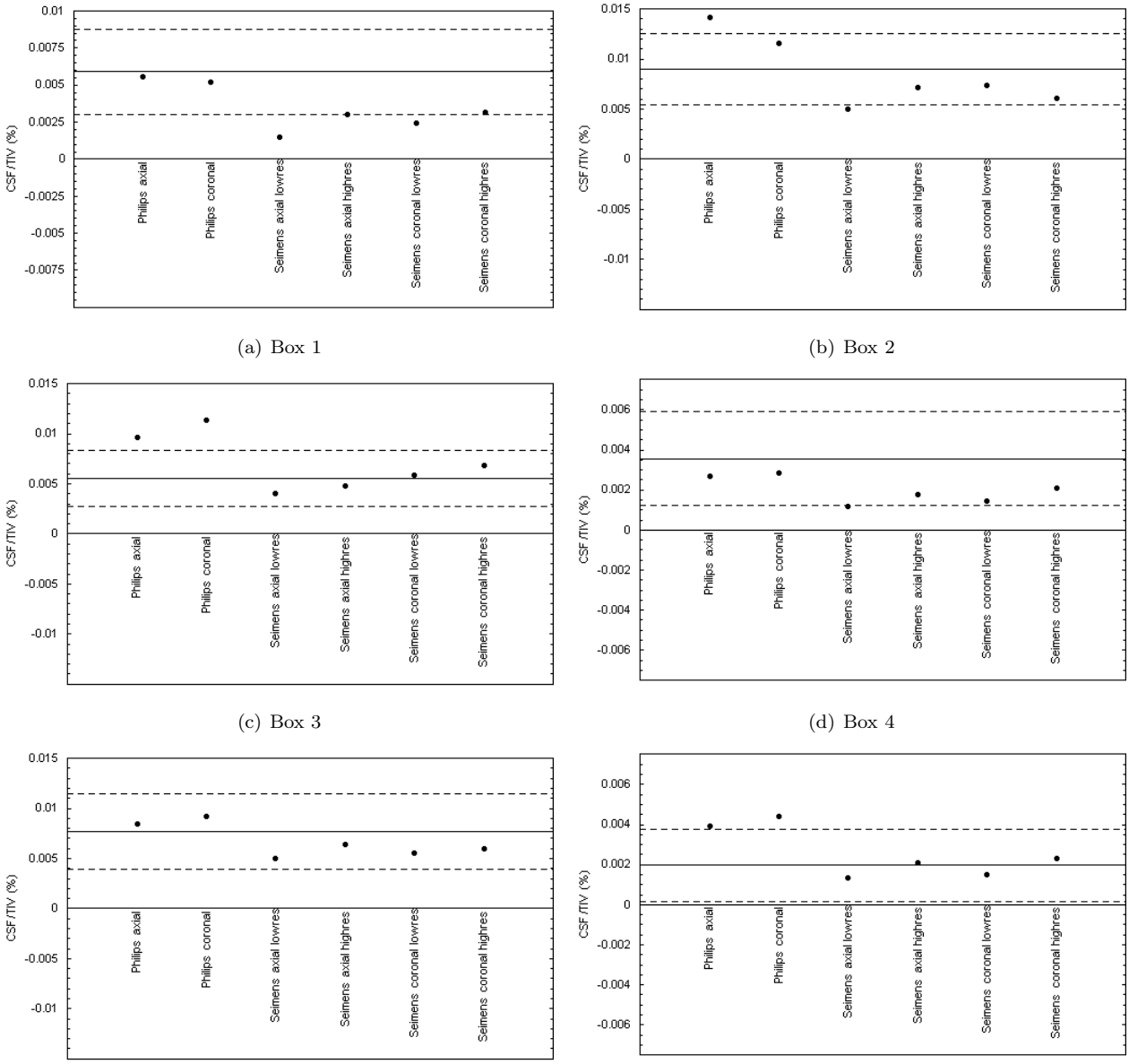

(a) Box 1

(b) Box 2

(c) Box 3

(d) Box 4

(e) Box 5

(f) Box 6

Figure 3: TIV normalised CSF volumes in the first six DODECANTS boxes. The solid line shows the expected value at the subject's age from the Weibull CDF fits described in TINA Memo no. 2004-002. The dashed lines show the upper and lower standard errors.

Image volume	Mean difference across boxes (s.d.'s)
Philips axial	0.607
Philips coronal	0.818
Siemens axial lowres	-0.974
Siemens axial highres	-0.453
Siemens coronal lowres	-0.641
Siemens coronal highres	-0.425

Table 4: The mean TIV normalised CSF volume differences across the 12 DODECANTS boxes between the values expected from the Weibull CDF fits described in TINA Memo no. 2004-002 and the measurements obtained in this study, in units of the standard error on the fits, for each image volume.

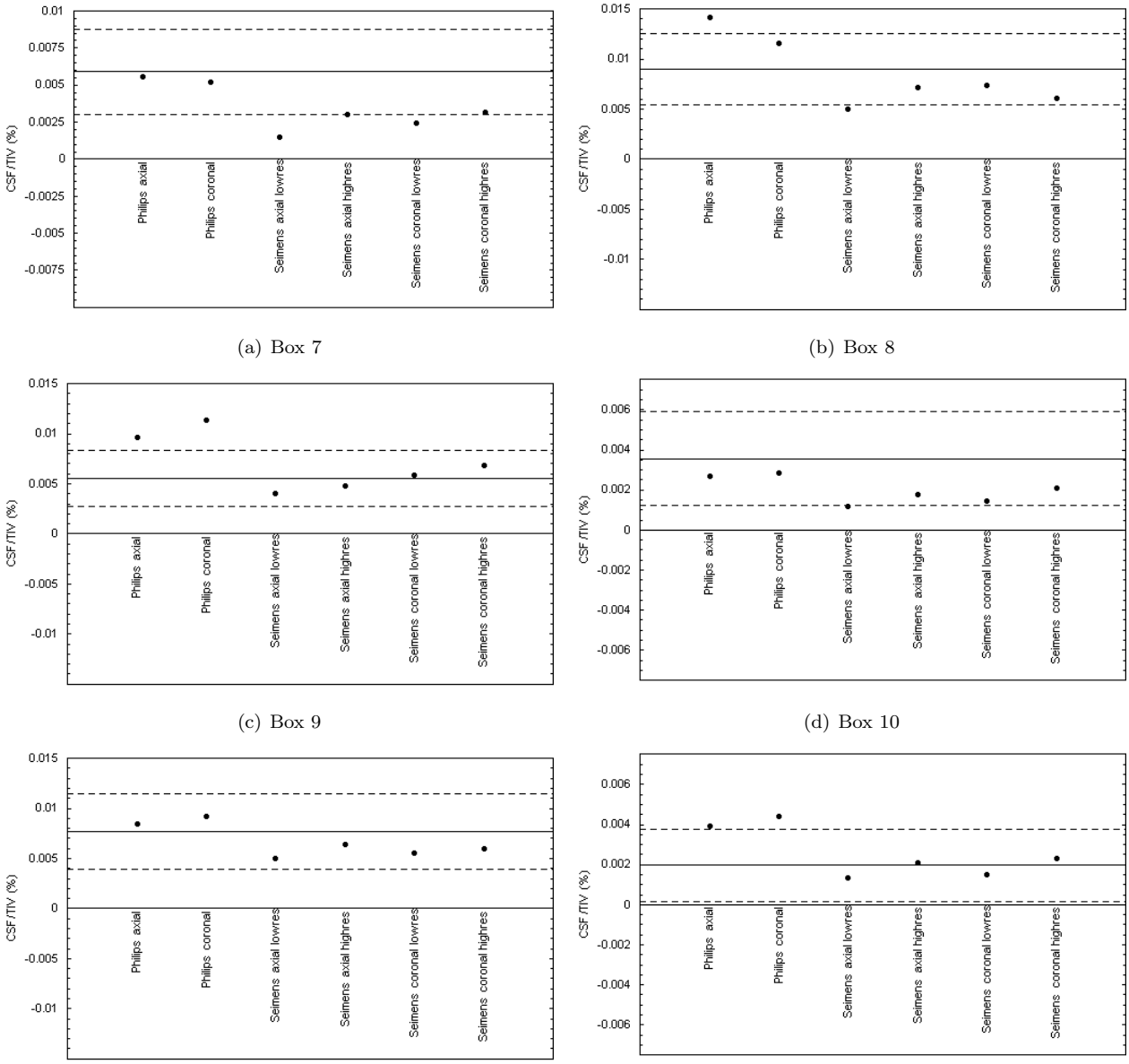

(a) Box 7

(b) Box 8

(c) Box 9

(d) Box 10

(e) Box 11

(f) Box 12

Figure 4: TIV normalised CSF volumes in the last six DODECANTS boxes. The solid line shows the expected value at the subject's age from the Weibull CDF fits described in TINA Memo no. 2004-002. The dashed lines show the upper and lower standard errors.

3 Discussion and Conclusions

Figure 2 and Table 3 indicate that the repeatability of TIV normalised CSF volume measurement across varying slice directions is typically lower than the biological variability across a cohort of normal subjects. The variability in volume measurement due to changes in protocol is however larger than this inherent biological variability. Figure 1 indicates that the variability seen between the protocols is consistent with the variability seen between the previous studies incorporated into the meta-study, implying that this is a result of the interaction between the segmentation algorithm and the protocol. The situation arises because the assumptions encoded in the segmentation algorithm, i.e. the assumed intensity model in the case of the present study, do not provide a perfect description of the intensity distribution of the data. A systematic error is therefore introduced in the CSF volume measurement, which is consistent across image volumes acquired using the same protocol, but which varies with changes in the shape of the intensity histogram i.e. varies as a function of scanner and scan parameters. Therefore, although the errors in transverse studies performed using a single protocol will be dominated by inherent biological variability, errors in such studies performed using image volumes from multiple protocols will be dominated by segmentation

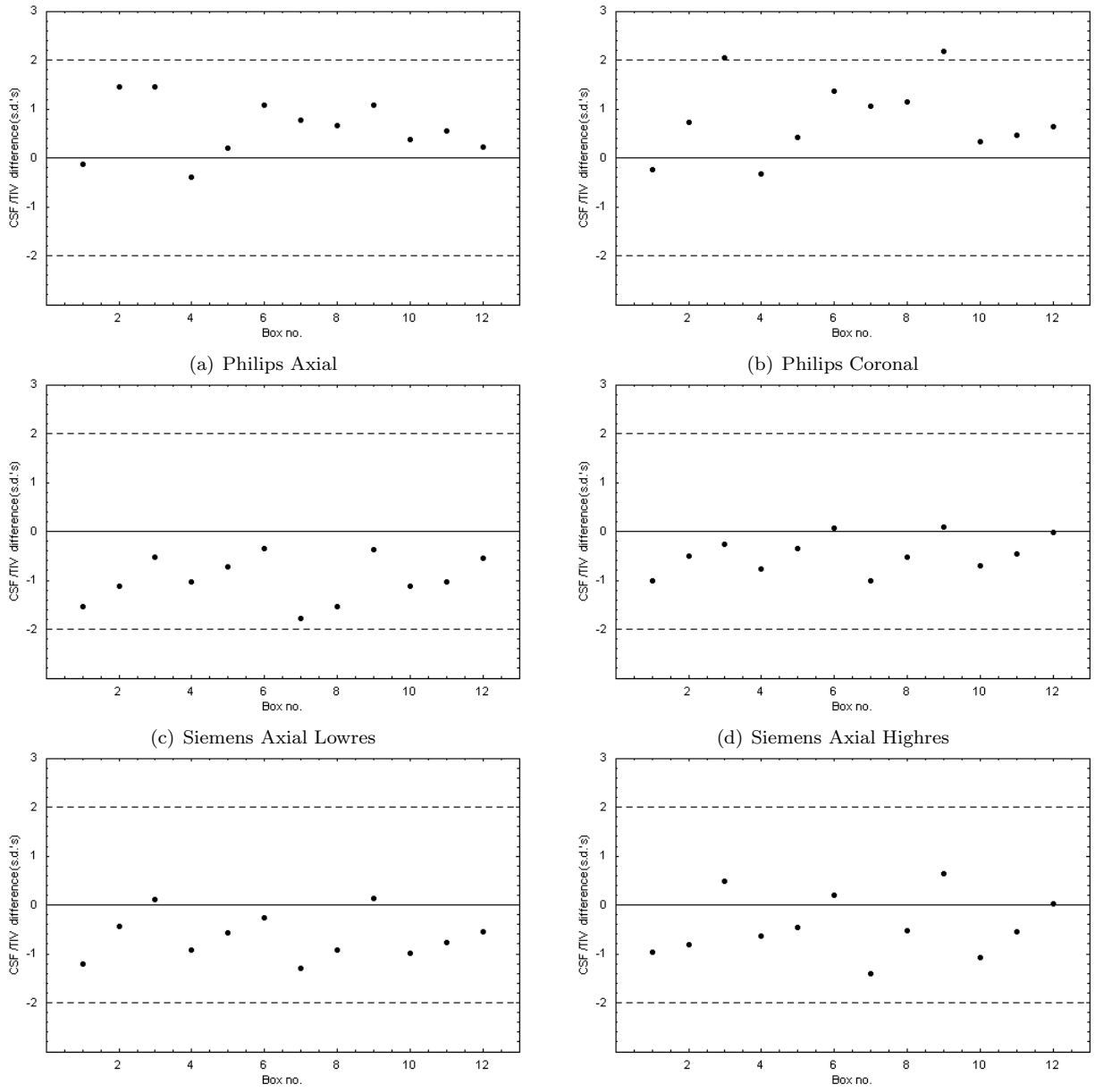

(a) Philips Axial

(b) Philips Coronal

(c) Siemens Axial Lowres

(d) Siemens Axial Highres

(e) Siemens Coronal Lowres

(f) Siemens Coronal Highres

Figure 5: The mean TIV normalised CSF volume differences across the 12 DODECANTS boxes between the values expected from the Weibull CDF fits described in TINA Memo no. 2004-002 and the measurements obtained in this study, in units of the standard error on the fits, for each image volume. The dashed lines show the upper and lower two standard deviation differences.

errors. This implies that image volumes from multiple protocols cannot be combined within a single study using the TINA DODECANTS technique.

Whilst the repeatability of the volume measurement across varying slice directions is satisfactory for the Philips and Siemens highres modalities, the results are poor for the Siemens lowres scans. Upon inspection it was determined that the intensity histogram for these scans lacked a clear peak for the CSF. The segmentation algorithm was therefore unable to fit the CSF reliably, requiring the use of gradient information in the segmentation in order to obtain the results given above. However, the intra-scan and inter-study variabilities in TIV normalised CSF volumes measured from these image volumes remains notable worse than the other protocols. Therefore the Siemens lowres protocol should not be used with the TINA DODECANTS technique.

The volume measurement results from the individual DODECANTS boxes are consistent with the above observations. Since the Weibull CDF fits from TINA Memo no. 2004-002 for the individual boxes are affected by registration errors (through errors on the positioning of the dividing planes) as well as segmentation errors, the

standard errors on the individual box fits are proportionately larger than the standard error on the fit to the overall CSF volume. Therefore, the results from the present study for the individual boxes are more consistent with the fits than is the case for the overall CSF volume. The best consistency was obtained using the Siemens highres protocol, implying that this protocol is suitable for use with the TINA DODECANTS algorithm.

Finally, it should be noted that the present study incorporated only a single subject, and the above conclusions should be interpreted in this light. Therefore, whilst the results presented here can be used to eliminate the possibility of using the Siemens lowres protocol with the DODECANTS technique, some reservations remain over recommending the Siemens highres protocol. Further study on a larger group of subjects would be required before it could be stated with any degree of confidence that this protocol is suitable for use with the DODECANTS technique.

References

[1] J Ashburner and K Friston. Multimodal image coregistration and partitioning-a unified framework. *NeuroImage*, 6:209–217, 1997.

[2] D D Blatter, E D Bigler, S D Gale, S C Johnson, C V Anderson, B M Burnett, N Parker, S Kurth, and S D Horn. Quantitative volumetric analysis of brain mr: Normative database spanning 5 decades of life. *American Journal of Neuroradiology*, 16:241–251, 1995.

[3] D Chan, N C Fox, R I Scahill, W R Crum, J L Whitwell, G Leschziner, A M Rossor, J M Stevens, L Cipolotti, and M N Rossor. Patterns of temporal lobe atrophy in alzheimer's disease. *Annals of Neurology*, 49:433–442, 2001.

[4] D T Chard, G J M Parker, C M B Griffin, A J Thompson, and D H Miller. The reproducibility and sensitivity of brain tissue volume measurements derived from an spm-based segmentation methodology. *JMRI*, 15:259–267, 2002.

[5] H E Cline, W E Lorensen, R Kinikis, and F Jolesz. Three-dimensional segmentation of mr images of the head using probability and connectivity. *Journal of Computer Assisted Tomography*, 14:1037–1045, 1990.

[6] C E Coffey, J A Saxton, G Ratcliff, R N Bryan, and J F Lucke. Relation of education to brain size in normal aging: Implications for the reverse hypothesis. *Neurology*, 53:189–196, 1999.

[7] M F Folstein, S E Folstein, and P R McHugh. "mini-mental state". a practical method for grading the cognitive state of patients for the clinician. *J Psychiatr Res*, 12:189–198, 1975.

[8] P A Freeborough, N C Fox, and R I Kitney. Interactive algorithms for the segmentation and quantitation of 3-d mri brain scans. *Comput. Methods Prog. Biomed*, 53:15–25, 1997.

[9] C D Good, I S Johnsrude, J Ashburner, R N A Henson, K J Friston, and R S J Frackowiak. A voxel-based morphometric study of ageing in 465 normal adult human brains. *NeuroImage*, 14:21–36, 2001.

[10] R C Gur, P D Mozley, S M Resnick, G L Gottlieb, M Kohn, R Zimmerman, G Herman, S Atlas, R Grossman, D Berretta, R Erwin, and R E Gur. Gender differences in age effect on brain atrophy measured by magnetic resonance imaging. *Proc. Natl. Acad. Sci. USA*, 88:2845–2849, 1991.

[11] J A Kaye, T Swihart, D B Howieson, A Dame, M M Moore, T Karnos, R M Camicioli, M Ball, B Oken, and G Sexton. Volume loss of the hippocampus and temporal lobe in healthy elderly persons destined to develop dementia. *Neurology*, 48:1297–1304, 1997.

[12] E Mueller, M M Moore, D C R Kerr, G Sexton, R M Camicioli, D B Howieson, J F Quinn, and J A Kaye. Brain volume preserved in healthy elderly through the eleventh decade. *Neurology*, 51:1555–1562, 1998.

[13] M Pokrić, N A Thacker, and A Jackson. The importance of partial voluming in multi-dimensional medical image segmentation. In *Proc. MICCAI*, pages 1293–1294, 2001.

[14] M Pokrić, N A Thacker, M L J Scott, and A Jackson. Multi-dimensional medical image segmentation with partial voluming. In *Proc. MIUA*, pages 77–80, 2001.

[15] R A Robb. A software system for interactive and quantitative analysis for biomedical images. In K H Hohne, H Fuchs, and D M Pizer, editors, *3D imaging in medicine*, volume F60, pages 333–361. NATO ASI Series, 1990.

[16] N A Thacker, M Pokrić, and D C Williamson. Noise filtering and testing illustrated using a multi-dimensional partial volume model of mr data. In *Proc. BMVC*, pages 909–919, Kingston, London, 2004.

[17] J L Whitwell, W R Crum, H C Watt, and N C Fox. Normalisation of cerebral volumes by use of intracranial volume: Implications for longitudinal quantitative mr imaging. *American Journal of Neuroradiology*, 22:1483–1489, 2001.